Journal of Power Sources 185 (2008) 118–128

Contents lists available at ScienceDirect

Journal of Power Sources

journal homepage: www.elsevier.com/locate/jpowsour

# Transient response of a unit proton-exchange membrane fuel cell under various operating conditions

Junhyun Cho, Han-Sang Kim, Kyoungdoug Min*

*School of Mechanical and Aerospace Engineering, Seoul National University, Seoul, South Korea*

ARTICLE INFO

*Article history:*
Received 11 March 2008
Received in revised form 21 May 2008
Accepted 5 June 2008
Available online 6 July 2008

*Keywords:*
Proton-exchange membrane fuel cell
Transient response
Dynamic behaviour
Visualization
Cathode flooding

ABSTRACT

The transient response of proton-exchange membrane fuel cells (PEMFCs) is an important criterion in their application to automotive systems. Nevertheless, few papers have attempted to study experimentally this dynamic behaviour and its causes. Using a large-effective-area (330 $cm^2$) unit PEMFC and a transparent unit PEMFC (25 $cm^2$), systematic transient response and cathode flooding during load changes are investigated. The cell voltage is acquired according to the current density change under a variety of stoichiometry, temperature and humidity conditions, as well as different flooding intensities. In the case of the transparent fuel cell, the cathode gas channel images are obtained simultaneously with a CCD imaging system. The different levels of undershoot occur at the moment of load change under different cathode stoichiometry, both cathode and anode side humidity and flooding intensity conditions. It is shown that undershoot behaviour consists of two stages with different time delays: one is of the order of 1 s and the other is of the order of 10 s. It takes about 1 s for the product water to come up on to the flow channel surface so that oxygen supply is temporarily blocked, which causes voltage loss in that "undershoot". The correlation of dynamic behaviour with stoichiometry and cathode flooding is analyzed from the results of these experiments.



## 1. Introduction

The proton-exchange membrane fuel cell (PEMFC) is considered to be the best alternative to the internal combustion engine in automotive applications due to its low operating temperature (under 80 °C), high power density and high efficiency. Nevertheless, PEMFCs have some issues that have to be solved before entering real application in automotive systems. The primary goal is to achieve fast and stable dynamic operation in response to drivers' power requirements such as start-up, acceleration, and deceleration.

While most of the studies regarding PEMFCs have focused on steady-state behaviour, several papers have recently studied dynamic behaviour. The majority of this research involves numerical simulation studies. Ceraolo et al. [1] developed a simplified, one-dimensional, dynamic model of a PEMFC based on MATLAB/SIMULINK®. Shan and Choe [2] predicted the transient response of a PEMFC to an electric load. The model separated the fuel cell into several components, namely: membrane, catalysts, gas-diffusion layer (GDL) and bipolar plates. Song et al. [3] examined the transient behaviour of water transport in the cathode gas-diffusion layer using a one-dimensional, non-isothermal, two-phase transient PEMFC model. By developing a three-dimensional dynamic model of the PEMFC, Wang et al. [4] showed that it took about 10 s for the cell to reach a new steady-state condition and that the main cause of the behaviour was the effect of water accumulation in the membrane. They also studied transient phenomena under current density step changes, with a focus on dry cell operation [5]. They concluded that a step increase in the current density instantaneously dries out the anode under the influence of an electro-osmotic drag. That study, however, focused solely on a single-channel model instead of the conventional cell configuration. In a recent paper [6], the same group developed a two-phase transient model and analyzed the dynamics of GDL dewetting and its impact on PEMFC performance. Yan et al. [7] studied the effects of gas channel type and the porosity of the GDL on the dynamic performance of a PEMFC using a two-dimensional mass transfer model of the cathode side. Shimpalee et al. [8–10] estimated undershoot/overshoot behaviour of a PEMFC under a fixed stoichiometry condition by using a three-dimensional model simulation. They recently predicted dynamic behaviour with a modified model that incorporates water phase change. Kumar and Reddy [11] studied the steady- and transient-state performance of a PEMFC for different gas-flow channel shapes. The results showed that it took about 10 s for the fuel cell to reach a new steady-state after a load change. Mueller et al. [12] developed a quasi-three-dimensional dynamic model for controlling a PEMFC. The spatial dynamic behaviour of

* Corresponding author. Tel.: +82 2 880 1661; fax: +82 2 883 0179.
*E-mail address:* kdmin@snu.ac.kr (K. Min).

0378-7753/$ – see front matter © 2008 Elsevier B.V. All rights reserved.
doi:10.1016/j.jpowsour.2008.06.073

current, water flux, species mole fractions and fuel cell temperature were presented.

By contrast, few papers have experimentally analyzed the transient response of a PEMFC. Kim et al. [13–15] performed experimental research on the undershoot/overshoot behaviour of PEMFCs under different stoichiometry conditions. They also demonstrated the effects of fuel dilution and hydrogen reservoir on the dynamic performance of PEMFCs. In addition, they investigated the effect of channel type on the transient response. Yan et al. [16] repeated various experimental results on the dynamic behaviour of a PEMFC under different temperatures, humidities, flow rates and flow channel type conditions. Nevertheless, specific experimental conditions were not defined clearly, and their study was somewhat limited due to the lack of analysis of the causes of dynamic behaviour. Recently, several papers have addressed the experimental relationship between membrane resistance and dynamic performance. Weydahl et al. [17] analyzed the transient response of a single PEMFC through resistance step measurements assisted by electrochemical impedance spectroscopy (EIS) and chronoamperometry. Takaichi et al. [18] measured the dynamic change of specific resistances of PEMFCs at various positions.

The above studies were concerned only with small fuel cells with an effective area of 5–25 $cm^2$, or even single-channel cells, because of difficulties associated with meshing and computing. Consequently, these studies were limited with respect to real automotive applications because many companies use fuel cells with an effective area of 200–350 $cm^2$. Due to the difficulty in real time data acquisition and modelling of two-phase flow, many papers have presented only simulation work without considering gas–liquid phase behaviour. Furthermore, parametric studies or reports of transient behaviour are rare.

The objectives of this study are to analyze the characteristics of the transient response of a PEMFC and to determine 'through experimental methods' the operating parameters that influence the transient response. First, using a 330 $cm^2$ large fuel cell, dynamic behaviour was investigated under various stoichiometries, load changes, temperatures, and humidity conditions to determine how operating conditions affect the transient response of a real automotive-size fuel cell. A direct visualization study using a 25 $cm^2$ transparent unit fuel cell was then performed to find the relationship between the transient response and the two-phase flow in that cathode flooding. The transparent unit fuel cell is made into a conventional lab scale-sized cell. With this series of experiments, this work attempts to determine which operating conditions and water transfer mechanisms influence the transient response of PEMFCs.

## 2. Experiment

### 2.1. Fuel cells and test station

#### 2.1.1. Large-effective-area PEMFC

The large PEMFC has effective area of 330 $cm^2$ (width: 234 mm, height: 141 mm) with a parallel serpentine channel (1 mm × 1 mm) flow pattern. Its membrane thickness is 30.48 μm and the equivalent weight of the dry membrane is 800. It has a coolant channel, and the operating temperature is controlled by a water circulation system.

The fuel cell is tested on a station that can accommodate up to 5 kW. Fig. 1 shows is schematic diagram of the test station for a 330 $cm^2$ fuel cell. High-purity hydrogen (99.999%) and high-purity air are supplied, and high-purity nitrogen is used to purge between experimental runs. The temperature of the whole gas line is controlled by a PID controller (Yokogawa Inc.). Humidity is controlled by a membrane humidifier at both the anode and cathode sides and is also monitored using a humidity sensor. The cell current is controlled by an electric loader (AMREL Inc.). The cell voltage acquisition system consists of a USB 6009 (National Instrument) board and LabVIEW program. The cell voltage data are obtained at 100 Hz and analyzed by using a LabVIEW-based program.

#### 2.1.2. Transparent PEMFC

Fig. 2 shows the unit transparent fuel cell used for the visualization experiment. A more detailed description of this transparent fuel cell is presented in [19]. A window is used at the cathode side for direct visualization of cathode flooding. A parallel serpentine gas-flow channel is fabricated using a thin carbon composite machined sheet (thickness: 1 mm) combined with an acrylic window. A conventional carbon bipolar plate with a parallel serpentine flow channel design is used at the anode side (0.8 × 1 mm). Hydrogen and air are supplied to the cell in a counter flow pattern for more efficient mass transfer. The membrane used in this study is Nafion® 112, which has a thickness of 50.8 μm and an effective area of 25 $cm^2$. To provide a good electrical connection, the current-collector is coated with gold on both the anode and the cathode sides. In addition, a cooling fin and cooling fan are used to control the operating cell temperature. The cooling fan speed is controlled as the cell temperature changes so that the reaction heat is removed more efficiently.

This transparent fuel cell is tested on another station that can accommodate up to 1 kW. Most of components, except the humidifier, are the same as those in the station described in the previous section. In this test station, a bubbling-type humidifier is used and the image acquisition system is constructed with a CCD camera (Lumenera Inc.) and Nikon Micro 60 mm lens (Nikon Inc.). The cathode channel images are transferred to a PC and saved once per second during the transient operations.

### 2.2. Experimental conditions

#### 2.2.1. Experiments with large-effective-area PEM fuel cell

In this study, the transient response is defined as the voltage response obtained as a result of a sudden step change in current. Steady-state performance data were initially obtained to determine the current value. The results are presented in Fig. 3 for the following conditions: current density change at a temperature of 70 °C, pressure of 1 bar, anode/cathode humidity of 100/100%, anode/cathode stoichiometry of (1) 1.2/2.0; (2) 2.4/2.0; (3) 1.2/4.0. The conditions of 100 A (0.3 A $cm^{-2}$) and 330 A (1 A $cm^{-2}$) current were chosen and the voltage response was analyzed under different stoichiometric conditions. However, at low temperature and low humidity conditions, there was a severe performance decrease at high current density, so that only the effects of temperature and humidity on the transient performance could not be interpreted. Therefore, currents of 100 and 200 A (0.6 A $cm^{-2}$) were chosen in these cases. These data are summarized in Table 1 and Fig. 4.

To analyze the influence of operating parameters on the transient response characteristics of a large-effective-area fuel cell, different experimental conditions were selected, as shown in Table 2.

The transient voltage response was obtained under different stoichiometric conditions and the current was step-changed between 100 and 330 A to determine the effect of stoichiometry on the transient response of the fuel cell. Gas-flow rates have to be changed as the current density is changed to maintain constant stoichiometry. However, it is impossible to change the flow rate suddenly using a mass-flow controller because of the physical limits of flow velocity, length of the gas line, and so forth. Therefore, in this work, the flow rate was maintained constant and the stoichiometry was changed before and after the load change. For example, if the flow rates were

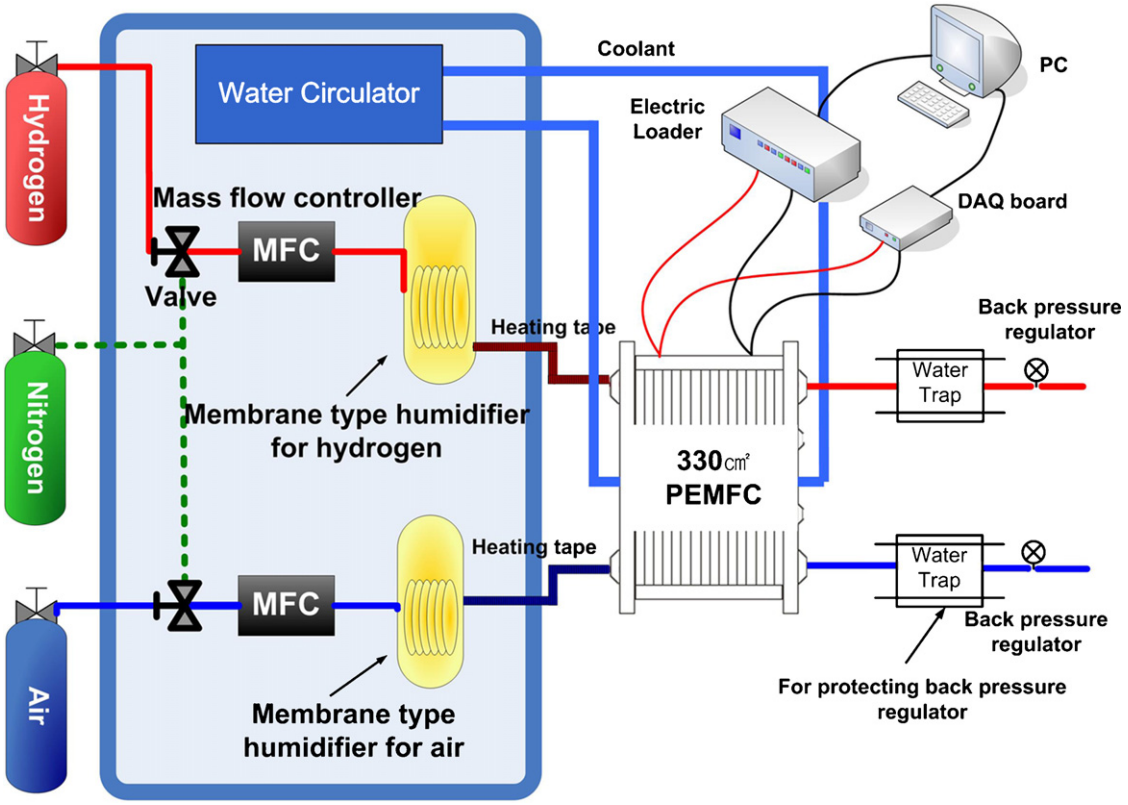


**Fig. 1.** Experimental apparatus for testing 330 $cm^2$ PEMFC.

fixed at 3.6/14.2 (lpm: liter per minute) at the anode/cathode side to maintain a stoichiometry of 1.2/2.0 at the 1 A $cm^{-2}$ load condition, these flow rates corresponded to the stoichiometry of 2.4/4.0 at the 0.5 A $cm^{-2}$ load condition. Table 3 shows these different stoichiometric conditions. The starved condition was set at 80% (1.0/1.6) of stoichiometry (1.2/2.0). The operating temperature and the humidity were maintained at 70 °C and 100% at both sides and pressure was fixed at 1 bar.

To determine the influence of load change on the transient voltage response, the current was changed from 100 to 200 A to represent a 50% power change. An excess-to-normal stoichiometry of 1.2/2.0 at the anode/cathode side at high load operation, an oper-

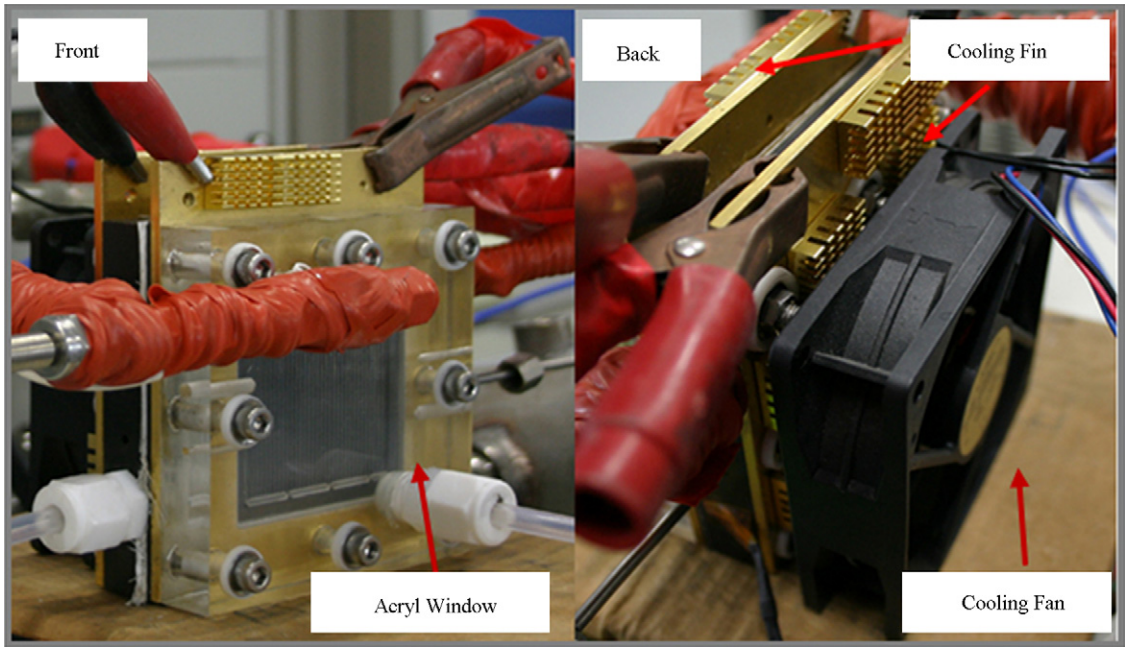


**Fig. 2.** Unit transparent PEMFC used in this study.

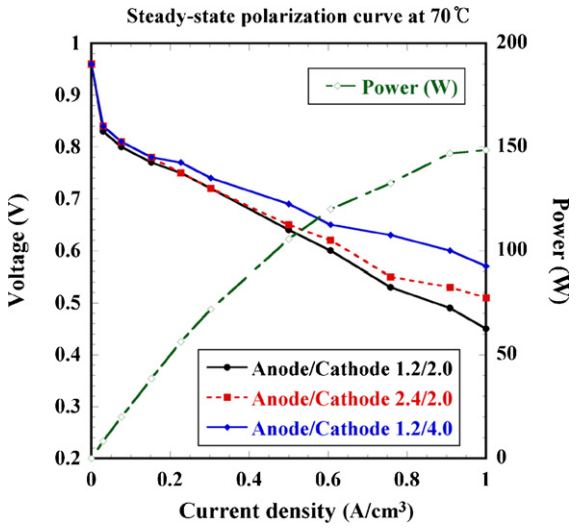


**Fig. 3.** Steady-state polarization curve for 330 $cm^2$ fuel cell under various stoichiometric conditions at 70 °C, a humidity of 100/100% and a pressure of 1 bar.

**Table 1**
Steady-state voltage and power data corresponding to current at each fuel cell

| Current (A) | Current density ($A\,cm^{-2}$) | Voltage (V) | Power (W) |
|---|---|---|---|
| 330 $cm^2$ cell | | | |
| 100 | 0.303 | 0.72 | 75 |
| 200 | 0.606 | 0.6 | 114 |
| 330 | 1 | 0.45 | 148.5 |
| 25 $cm^2$ cell | | | |
| 7.5 | 0.3 | 0.7 | 5.25 |
| 15 | 0.6 | 0.54 | 8.1 |

ating temperature of 70 °C, a humidity of 100% at both sides, and a pressure of 1 bar were maintained.

To evaluate the influence of operating temperature on the transient voltage response, the cell voltage was measured for a current step change from 100 to 200 A and from 200 to 100 A at temperatures of 30, 40, 50, 60 and 70 °C. The flow rate was fixed to maintain a stoichiometry of 1.2/2.0 (anode/cathode) at 200 A load. A fully-hydrated gas condition and a pressure of 1 bar were also maintained.

Finally, to determine the influence of humidity on the transient voltage response, different levels of humidity of hydrogen and

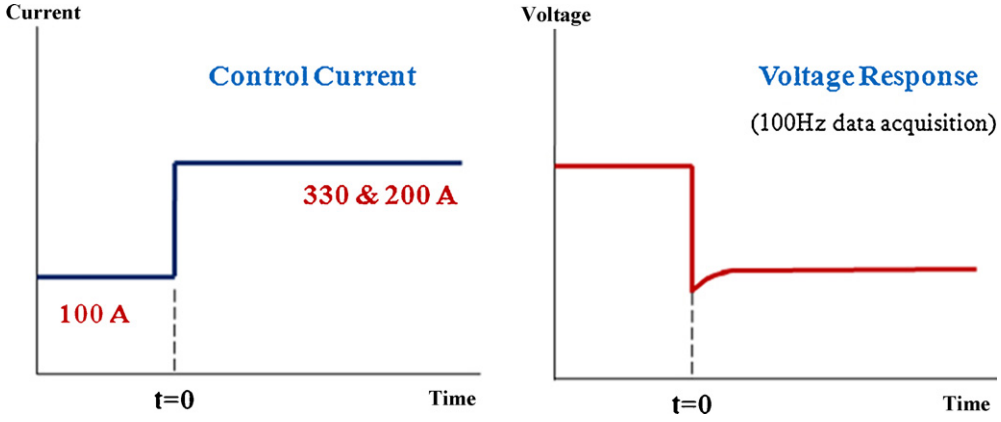


**Fig. 4.** Sudden step change of current for large fuel cell (low-load-to-high-load).

**Table 2**
Experimental conditions for large-effective-area fuel cell

| Variable | Load change | Stoichiometry | | Humidity (%) | | Temperature (°C) | Pressure (bar) |
|---|---|---|---|---|---|---|---|
| | | Anode | Cathode | Anode | Cathode | | |
| Stoichiometry | 100A → 330A | 1.2<br>2.4<br>1.2 | 2.0<br>2.0<br>4.0 | 100 | 100 | 70 | 1 |
| | 330A → 100A | 1.0<br>1.2<br>1.0 | 2.0<br>1.6<br>1.6 | | | | |
| Load change | 100A → 200A | 1.2<br>2.4<br>1.2 | 2.0<br>2.0<br>4.0 | | | | |
| Temperature | 100A → 200A | 1.2 | 2.0 | | | 30,40,50,60,70 | |
| Humidity | 100A → 200A | | | 100<br>50 | 100<br>100 | 70 | |
| | 200A → 100A | | | 100<br>50 | 50<br>50 | | |

**Table 3**
Case of experiments for different flow rates and stoichiometries

| | Flow rate (Lpm) | | Stoichiometry | | Stoichiometry | |
|---|---|---|---|---|---|---|
| | Hydrogen | Air | Hydrogen | Air | Hydrogen | Air |
| 100–330 A | | | | | | |
| | 3.577 | 14.194 | 3.96 | 6.60 | **1.20** | **2.00** |
| Excess to normal | 7.154 | 14.194 | 7.92 | 6.60 | **2.40** | **2.00** |
| | 3.577 | 28.388 | 3.96 | 13.20 | **1.20** | **4.00** |
| | 2.981 | 11.355 | 3.30 | 5.28 | **1.00** | **1.60** |
| Excess to starved | 3.577 | 11.355 | 3.96 | 5.28 | **1.20** | **1.60** |
| | 2.981 | 14.194 | 3.30 | 6.60 | **1.00** | **2.00** |
| 330–100 A | | | | | | |
| | 3.577 | 14.194 | **1.20** | **2.00** | 3.96 | 6.60 |
| Normal to excess | 7.154 | 14.194 | **2.40** | **2.00** | 7.92 | 6.60 |
| | 3.577 | 28.388 | **1.20** | **4.00** | 3.96 | 13.20 |
| | 2.981 | 11.355 | **1.00** | **1.60** | 3.30 | 5.28 |
| Starved to excess | 3.577 | 11.355 | **1.20** | **1.60** | 3.96 | 5.28 |
| | 2.981 | 14.194 | **1.00** | **2.00** | 3.30 | 6.60 |

air gas such as 50 and 100%, respectively, were used. The voltage response was analyzed for a sudden step change of current from 100 to 200 A at a temperature of 70 °C, a pressure of 1 bar and a stoichiometry of 1.2/2.0.

#### 2.2.2. Experiments with transparent PEMFC

Table 4 shows the experimental conditions for the transparent unit cell experiments. In all cases, the experiments were conducted at a temperature of 40 °C, a hydrogen stoichiometry of 1.2, an anode/cathode humidity of 100/100% and a pressure of 1 bar. The steady-state polarization curve of the transparent unit cell was obtained and the results are summarized in Table 1.

At first, to compare with the results of the large-effective-area fuel cell experiments, the voltage response of the fuel cell was obtained under different stoichiometric conditions as was done in the case of the large-effective-area fuel cell experiments during a 7.5–15 A step change in current. The flow rate was fixed so as to maintain the stoichiometry at the high load (15 A) condition. The cathode stoichiometry condition was varied at 2.0 (normal), 1.6 (starved) and 4.0 (excess). Hydrogen stoichiometry was fixed at the 1.2 (normal) condition. Not only the voltage response of the fuel cell but also the cathode channel image was obtained during the transient operation to analyze the relationship between the cell voltage response performance and the water appearance on the flow channel surface.

Second, to analyze the effect of the mass transfer limit on the transient response, different levels of flooding were enforced by controlling the operating time as 10 and 300 s before a load change. The flow rate of the cathode side was fixed at a stoichiometry of 1.6 at the high load condition. The voltage response was recorded according to a sudden step change in current density, i.e., 0.3 A $cm^{-2}$ (7.5 A) to 0.6 A $cm^{-2}$ (15 A).

## 3. Results and discussion

### 3.1. Transient response of large-effective-area PEMFC under various operating conditions

Fig. 5(a) and (b) show the transient voltage response of a large-effective-area cell when the current is changed from 100 to 330 A under various stoichiometric conditions. A voltage undershoot behaviour is observed after a load change. Fig. 5(a), the case representing a sufficient amount of gas supply, shows that it takes about 50 s to reach a new steady-state condition with a stoichiometry of 1.2/2.0, and 40 s and 20 s with a stoichiometry of 2.4/2.0 and 1.2/4.0, respectively. This time delay is much longer than the results from previous papers [8–10,13–15]. This result is due to severe water flooding, which interferes with the mass-transfer process; however, simulations were not capable of identifying this phenomenon. In the case of 1.2/2.0 stoichiometry, the voltage decreases continuously after reaching its maximum level. By contrast, when the cathode stoichiometry is 4.0, the voltage remains at the maximum level. This result suggests that long-term voltage loss (as in the 1.2/2.0 case) occurs due to the mass-transfer limit of oxygen by cathode flooding at sustained high-load operation. An enlarged graph given in the inset of Fig. 5(a) shows that the voltage does not recover immediately but rather decreases continuously for about 2 s after a load change. Also, the time to reach the minimum voltage level decreases as the stoichiometry, especially the cathode stoichiometry, increases.

**Table 4**
Experimental conditions for transparent fuel cell

| Variable | Load change | Stoichiometry | | Humidity (%) | | Temperature (°C) | Pressure (bar) |
|---|---|---|---|---|---|---|---|
| | | Anode | Cathode | Anode | Cathode | | |
| Stoichiometry | 7.5A → 15A | 1.2 | 1.6<br>2.0<br>4.0 | 100 | 100 | 40 | 1 |
| Initial Flooding | 7.5A (300s) → 15A | 1.2 | 1.6 | | | | |
| | 7.5A (10s) → 15A | | | | | | |

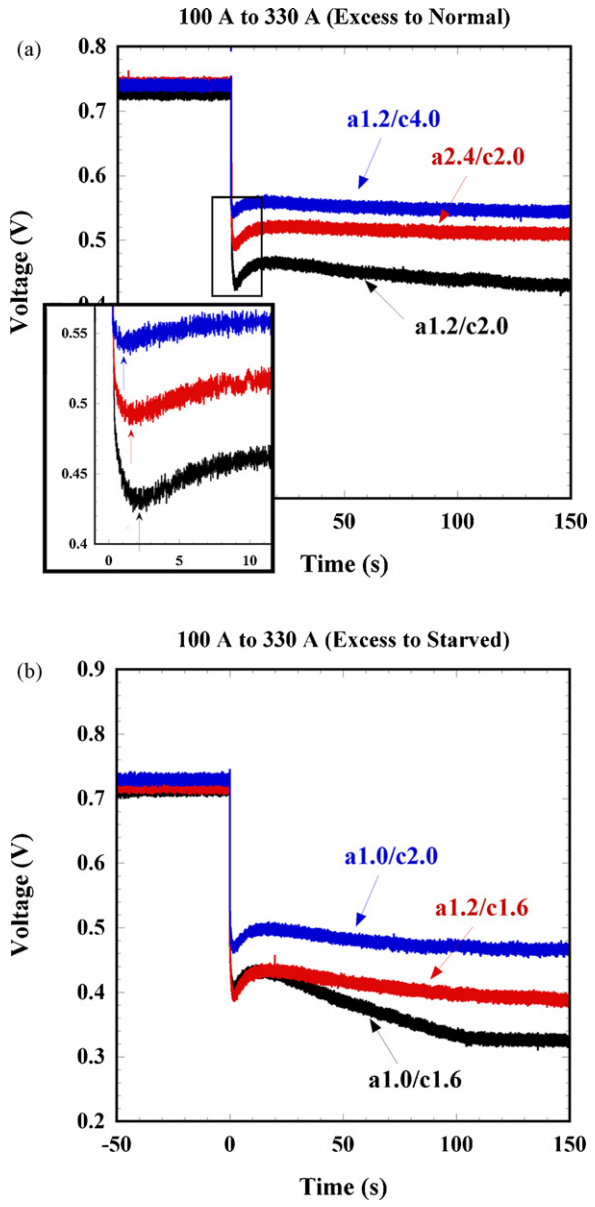


**Fig. 5.** Voltage response as current is changed from 100 to 330 A under (a) excess-to-normal and (b) excess-to-starved stoichiometric conditions, at a temperature of 70 °C, a humidity of 100/100%, and a pressure of 1 bar.

The schematic of this undershoot behaviour is illustrated in Fig. 6. When the load changes from a low to a high level, the voltage response exhibits two different time delays until it reaches a new stead-state. The first time delay, which is of the order of 1 s, is the time that the voltage decreases continuously until it reaches the minimum level. The second delay, which is on the order of 10 s, is the time until the voltage reaches the new steady-state level. The fact that the first time delay decreases as the stoichiometry increases, from Fig. 5(a), suggests that the gas convection and diffusion process is related to the first time delay. The time to penetrate the GDL for gas is calculated as:

$$\tau_k = \frac{\delta_{GDL}^2}{D_g^{eff}} \quad (1)$$

Since the GDL thickness $\delta_{GDL}$ is around 0.3 mm and the general diffusivity $D_g^{eff}$ of porous GDL is $10^{-5}$ m$^2$ s$^{-1}$, the time constant $\tau_k$ is of the order of 0.01 s [4]. In this experimental study, However, the

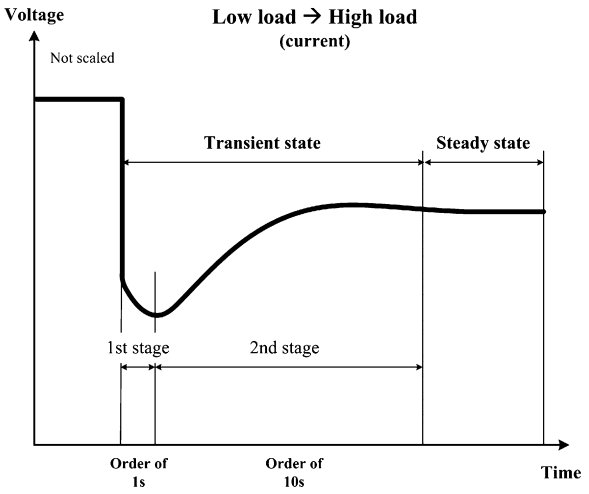


**Fig. 6.** Schematic of voltage undershoot behaviour during current step change (low-load-to-high-load).

time constant is of the order of 1 s. This difference is discussed in the latter part of this paper.

The second-stage time delay is due to the recovery of membrane water content. As the load changes to a high current density, the membrane dehydrates and its resistance correspondingly increases, which induces a voltage loss. In time, due to the supply of humidified gas and internal hydration from electro-osmotic drag and back diffusion, the membrane becomes hydrated, which results in voltage recovery. The membrane hydration time is estimated to be:

$$\tau_m = \frac{(\rho \delta_m \Delta\lambda)/EW}{I/2F} \quad (2)$$

Here, $\tau_m$ is the time constant for membrane hydration, $\rho$ is the membrane density, $\delta_m$ is the membrane thickness, $\Delta\lambda$ is the water content, EW is the equivalent weight of the membrane, $I$ is the current density and $F$ is the Faraday constant. Inserting typical values, the time constant is found to be of the order of 10 s [4].

From Fig. 5(a), the second time delay is shorter due to increased cathode stoichiometry from the efficient supply of humidified air into the membrane and active water removal in the flow channel. Based on this observation, it is concluded that more stable and faster transient operation is obtained under air-sufficient stoichiometry conditions.

Fig. 5(b) shows the results for the 80% stoichiometry condition (1.0/1.6) at 330 A (high load) operation. This result indicates that more severe dynamic behaviour arises under insufficient gas supply circumstances. The time to reach a new steady-state becomes longer and the amount of undershoot increases. Similar to Fig. 5(a), air stoichiometry has a much greater effect on the transient response than hydrogen stoichiometry.

Fig. 7 describes the voltage response when the current is changed from 330 to 100 A (high load to low load). The dynamic performance is more stable and faster than that of the opposite case. The time delay to reach a new steady-state is small, i.e., under 10 s. This faster response is due to the sufficiently hydrated membrane, active osmotic drag and back diffusion motion, and better performance of the mass transfer in the GDL during the high-load operation. These factors lead to better transient operation.

To evaluate the influence of load change on the transient response of the fuel cell, the current was changed from 100 to 200 A, and the results are illustrated in Fig. 8. Compared with Fig. 5(a), in which the current is changed from 100 to 330 A, Fig. 8 shows a similar trend of voltage response, such as a voltage loss just after a

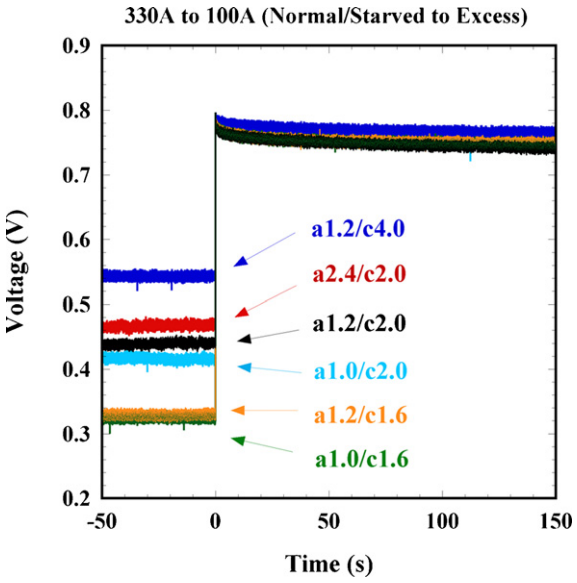


**Fig. 7.** Voltage response as current is changed from 330 to 100 A under normal-to-excess and starved-to-excess stoichiometric conditions, at a temperature of 70 °C, a humidity of 100/100 %, and a pressure of 1 bar.

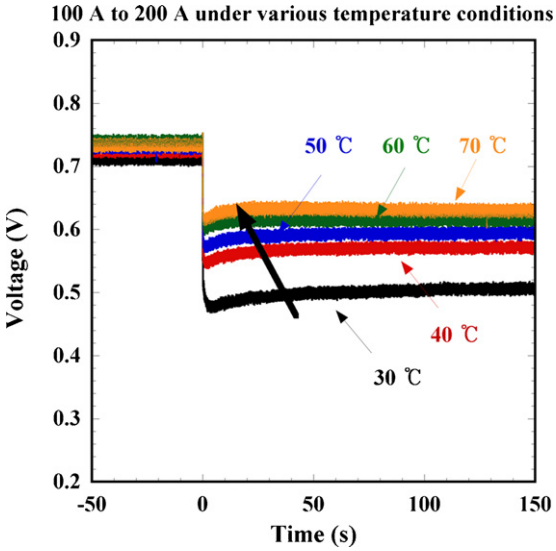


**Fig. 9.** Voltage response as current is changed from 100 to 200 A under various temperature conditions, excess-to-normal stoichiometry (1.2/2.0), humidity of 100/100%, and pressure of 1 bar.

load change. However, the magnitude of undershoot decreases as the amount of load change decreases. The voltage increases more rapidly to a new steady-state. Air stoichiometry is a more dominant factor than the hydrogen stoichiometry, as was demonstrated by the results of previous experiments. Based on this comparison, it is concluded that the mass-transfer limit of gas and water is a crucial factor for dynamic performance loss in high current density operation.

The transient response under different temperature conditions is shown in Fig. 9. The second-stage time delay becomes shorter as the operating temperature increases because the increased water activity enhances membrane conductivity.

Fig. 10(a) and (b) presents the effect of humidity on the transient voltage response. In the case of a load increase, Fig. 10(a) shows that

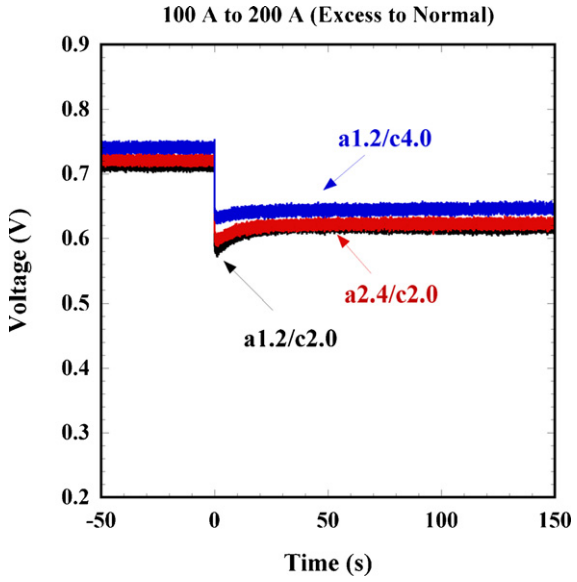


**Fig. 8.** Voltage response as current is changed from 100 to 200 A under an excess-to-normal stoichiometric condition, at a temperature of 70 °C, a humidity of 100/100%, and a pressure of 1 bar.

the humidity of both hydrogen and oxygen have to be maintained in a fully-hydrated state to achieve better transient operation. If there is not a sufficient supply of water during a load change, the membrane dehydrates and osmotic drag and back diffusion de-activate, which cause a decrease in membrane conductivity and mass transfer, and an eventual increase in voltage drop. There is a substantial time delay for water accumulation on the membrane compared with the electrochemical reaction time and gas-diffusion time, so voltage recovery is slow under the low humidity conditions. As oxygen and hydrogen continue to react and produce water, the membrane becomes hydrated and has low resistance. In the case of an anode/cathode humidity of 50/100%, the continuous back-diffusion process helps the recovery of the voltage loss up to a nearly fully hydrated condition. Based on the fact that the voltage loss increases at low humidity, this observation also supports the idea that the second-stage time delay shown in Fig. 6 is due to the time delay of water content build-up in the membrane.

On the other hand, in the case of high load to low load, Fig. 10(b) indicates that if the humidity at any one side is sufficient, there is a small overshoot and a fast response compared with the severe case (50/50%). This result can be interpreted as corresponding to a sufficient amount of water in the membrane during a high load operation, so that the dried cathode side recovers through osmotic drag from the hydrated anode side and the dried anode side recovers through back-diffusion motion from the cathode side. In the case of a 50/50% condition, the voltage decreases continuously due to the lack of water contained in the gases. This continuous voltage drop causes an overshoot in voltage response just after the load change. After some time, the voltage level finally reaches a new steady-state as the water masses from the low humidity gas and the product water in the fuel cell are electrochemically balanced.

From these experiments, the humidity of both sides for a load increase and any one side for a load decrease are a very important determinants of the transient response of a PEMFC.

In the series of experiments, undershoot behaviour is observed during low-load-to-high-load change and overshoot behaviour during high-load-to-low-load change. Undershoot behaviour is analyzed in more detail to distinguish two different time delays. In the first stage, the theoretical time delay is of the order of 0.01 s. In these experiments, however, the time delay is found to be of the

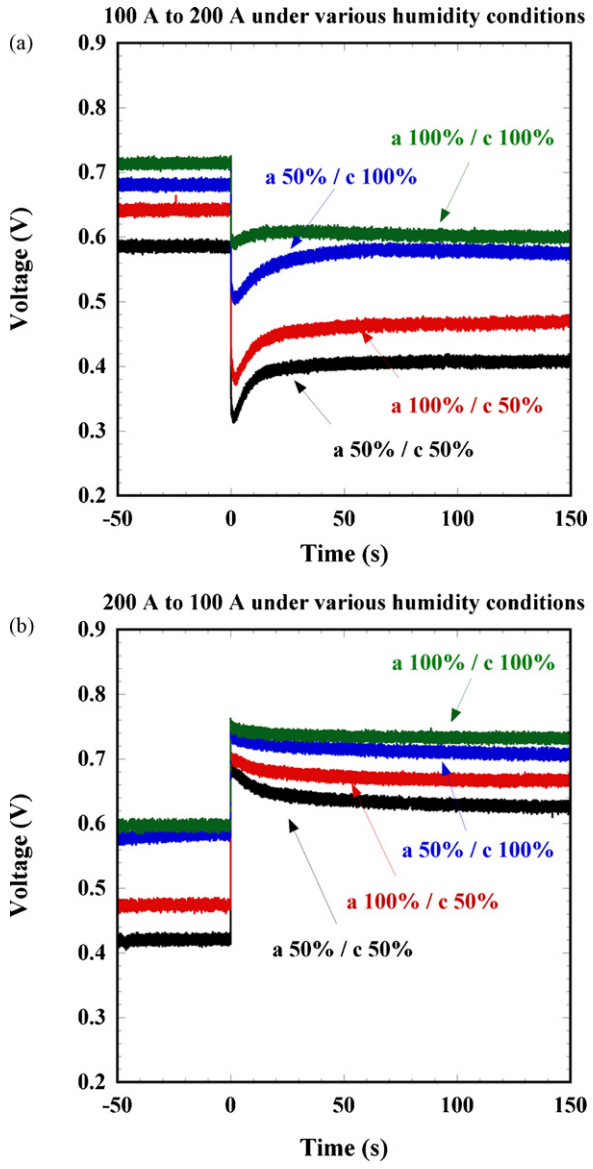


**Fig. 10.** Voltage response as current is changed from (a) 100 to 200 A; (b) 200 to 100 A under various humidity conditions, temperature of 70 °C, excess-to-normal stoichiometry (1.2/2.0), and pressure of 1 bar.

order of 1 s. To investigate further this difference in time delay, a visualization study was conducted simultaneously with the voltage performance data analysis.

### 3.2. Transient response of transparent unit cell

Fig. 11 shows the voltage response of a unit transparent fuel cell for a current change from 7.5 A (0.3 A cm$^{-2}$) to 15 A (0.6 A cm$^{-2}$) under an air stoichiometry of 1.6/2.0/4.0 at high load. Similar to previous experiments with the large-effective-area fuel cell, an undershoot behaviour is observed just after a load change. It takes about 50 s for voltage recovery and as the air stoichiometry increased, the voltage responses became more stable. As mentioned, this behaviour, is due to the two-phase motion of the liquid and gas phase that leads to the slow diffusion velocity of oxygen, the lack of uniformity of the oxygen concentration distribution, and inactive water removal. The enlarged graph in Fig. 11 shows that performance continuously decreases until around 0.1–1 s. Although there is a slight difference in time delay compared with

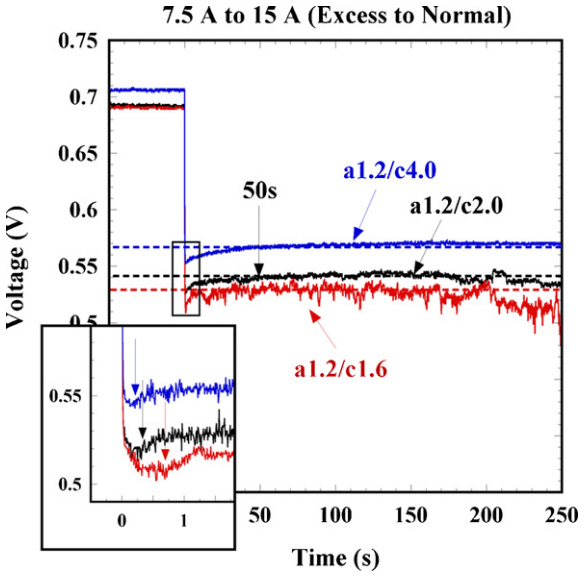


**Fig. 11.** Voltage response as current is changed from 7.5 to 15 A under different cathode stoichiometries of 1.6/2.0/4.0, temperature of 40 °C, humidity of 100/100%, and pressure of 1 bar.

the experiment result for the large-effective-area fuel cell due to the difference in the membrane and GDL thicknesses, Fig. 11 shows two different time delays as well. This indicates that these time delays come from through-plane direction behaviour from channel to membrane. In addition, because the undershoot is smaller than that of the large-effective-area fuel cell, the amount of undershoot is considered to be affected by the flow direction mass-transfer limit. Non-uniform oxygen and water content distribution causes spatial performance loss, which results in a substantial undershoot in the large-effective-area fuel cell as a result of summation of spatial loss.

The cathode gas channel images from 0 to 3 s after a load change at a cathode stoichiometry of 1.6 are given in Fig. 12. A steep increase in vapour (white colour in channel in images) is observed in the image after 2 s, which indicates that it takes about 1 s for the water produced at the catalyst layer to come up to the flow channel surface passing through the GDL. In other words, the product water remains in the GDL, blocking the pores for about 1 s. This observation of the mass-transfer process in the fuel cell is illustrated in Fig. 13. During the time that the supplied gas moves on to the triple phase boundary where the electrochemical reaction occurs, the increasing vapour and the condensed water suddenly block the GDL pores and this blockage interferes with mass transfer, causing a temporary performance decrease. Gas convection also decreases because the produced vapour also blocks the surface of the gas-flow channel. Therefore, the undershoot behaviour under transient operation is due to limitation of the gas-diffusion time delay. As mentioned, the time constant of gas penetration through the GDL is estimated to be of the order of 0.01 s. From Fig. 11, undershoot behaviour or a performance decrease is observed within about 1 s after the load change. The fact that the time order is 0.1–1 s coincides with the result of image analysis is that it takes more time for gas to be fed to the triple boundary layer compared with the theoretical value because of conflict behaviour between gas-in motion and gas or liquid-out motion of water. It is concluded that it takes about 1 s for this two-phase conflict motion to reach a new steady-state. In Fig. 5(a), which presents the result for a large-effective-area fuel cell, continuous voltage loss occurs for 2 s after the load change. This result can be interpreted from the same point of view as the transparent fuel cell analysis that considered two-phase mass-

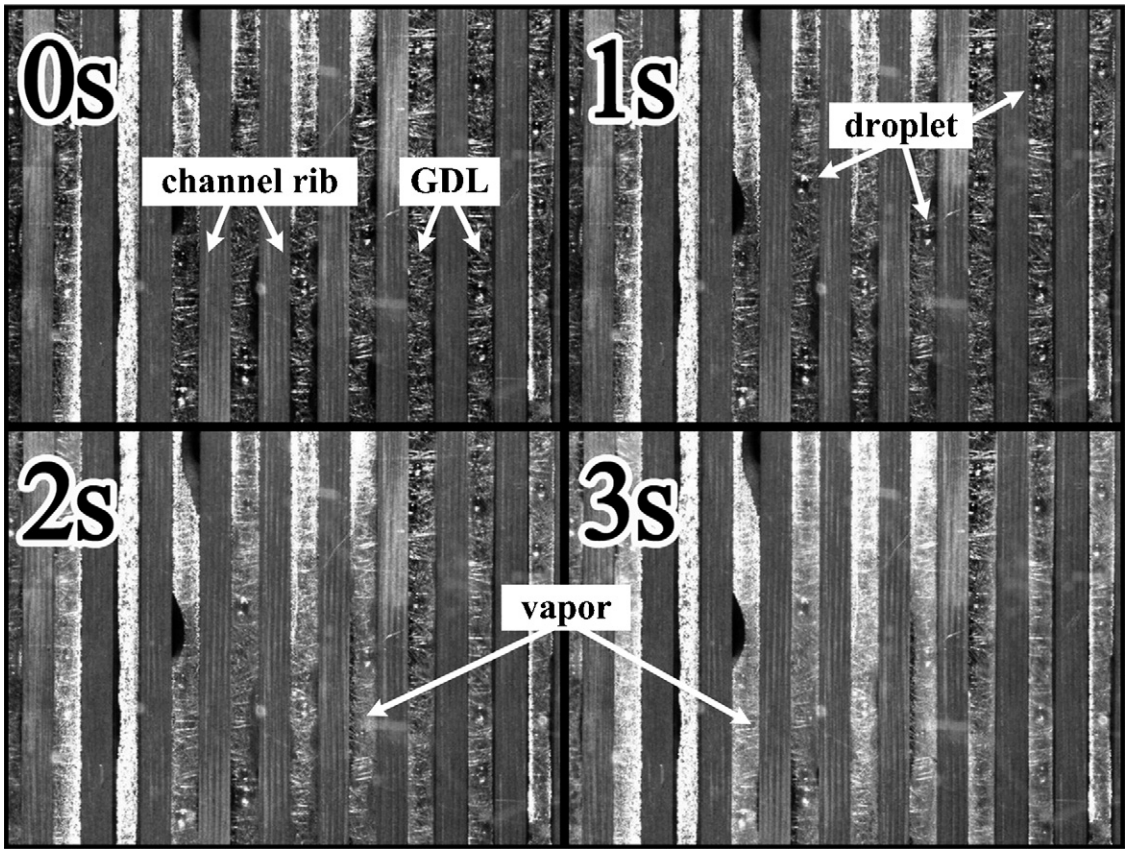


**Fig. 12.** Images of cathode channel flooding at cathode stoichiometry of 1.6, temperature of 40 °C, humidity of 100/100 %, and pressure of 1 bar.

transfer conflict motion. Moreover, the fact that more undershoot and a slow recovery time are obtained under low air stoichiometry conditions with both the large-effective-area and general lab-scale small-area fuel cells indicates that undershoot behaviour during low load-to-high load change operation occurs due to the delay of gas diffusion into the catalyst layer from the cathode flooding phenomenon. As the stoichiometry increases, convection and diffusion processes are improved and thereby yield a good dynamic performance from the fuel cell.

Finally, to investigate the influence of cathode flooding on the transient response, the operating time before load change was controlled. The channel image and voltage response data are shown in the Figs. 14 and 15, respectively. The images of cathode channel flooding at $t = 2$ s after a load change under low flooding intensity versus standard intensity is presented in Fig. 14. A smaller amount of water droplets or slugs are attached on the channel surface in the case of a low initial flooding intensity. Analysis of the voltage response result illustrated in Fig. 15 shows that not only does steady-state performance increase but also a better transient response is obtained with less undershoot and faster voltage loss recovery under a low flooding intensity condition, it can be concluded that the delay of oxygen supply and non-homogeneous

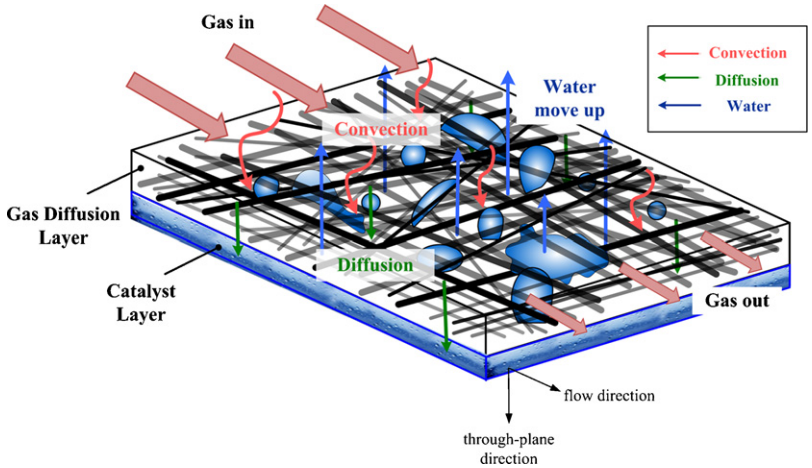


**Fig. 13.** Schematic of mass-transfer process in PEMFC.

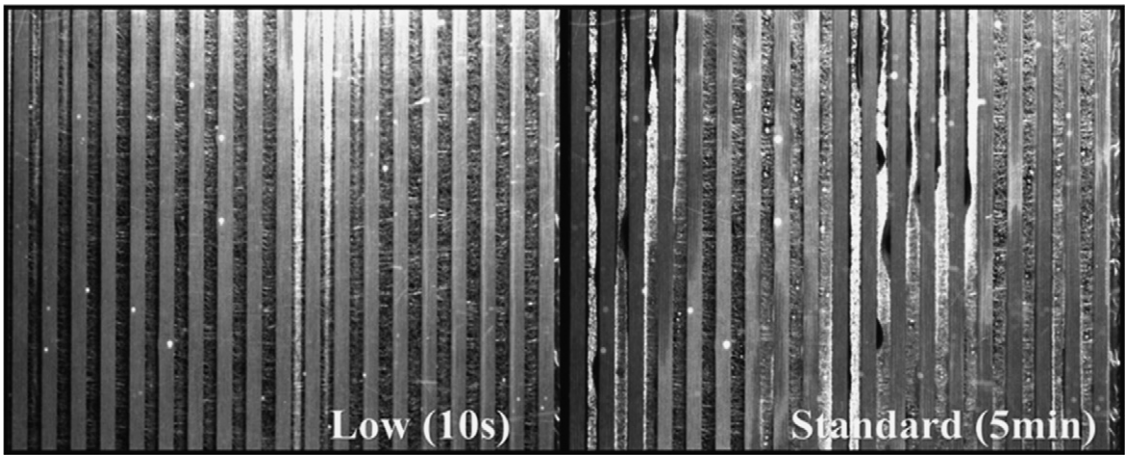


**Fig. 14.** Images of cathode channel flooding under different flooding intensities at $t = 2$ s after load change, cathode stoichiometry of 1.6, temperature of 40 °C, humidity of 100/100%, and pressure of 1 bar.

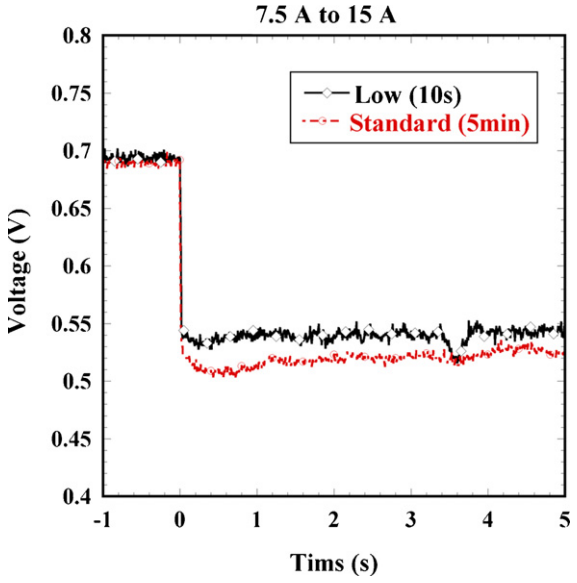


**Fig. 15.** Voltage response as current is changed from 7.5 to 15 A under different flooding intensities, cathode stoichiometry of 1.6, temperature of 40 °C, humidity of 100/100%, and pressure of 1 bar.

oxygen distribution in the channel and GDL due to flooding result in the decrease of dynamic performance.

## 4. Conclusions

An experimental study on the transient response of a PEMFC was conducted with direct visualization using a unit large-effective-area fuel cell (330 $cm^2$) and a unit transparent fuel cell (25 $cm^2$) under various operating conditions and flooding conditions. Through this research, several conclusions have been obtained.

(1) Both of the two PEMFCs exhibit undershoot/overshoot behaviour of voltage and time delay to reach a new steady-state after a sudden change of current load.
(2) In the case of low-load-to-high-load operation, undershoot is observed, and this response takes place in two stages, each of which has a different mechanism through analysis of the results from experiments under various stoichiometries, amounts of load change, temperatures and humidity conditions, as well as those reported in the literature.
(3) The first stage of time delay, which is on the order of 1 s, is due to through-plane gas convection and the diffusion mass-transfer limit. The time delay of the water content recovery of the membrane is of the order of 10 s and is described as a second-stage delay. In addition, by comparison of two cells that have different effective areas, the relationship between the undershoot level and the non-uniformity of gas and water content to the flow channel direction has been investigated. It is concluded that undershoot is due to the delay of oxygen supply, non-uniform oxygen distribution, cathode flooding and delay of water accumulation in the membrane.
(4) In the case of high-load-to-low-load operation, a fast response time of several seconds is observed because a sufficiently hydrated membrane, active osmotic drag and back-diffusion process, and better mass transfer are maintained during high-load operation.
(5) By using the unit transparent fuel cell, the relation between the transient response and the two-phase flow has been determined. Analysis of a series of channel images shows that it takes about 1 s for produced water or vapour to come out on the channel surface; this result coincides with the voltage undershoot behaviour.

This experimental research on the transient response of the PEMFC contributes to the evaluation of fuel cell modelling, the development of optimum cell design, and the construction of control logic and driving strategy for a fuel cell vehicle.

## Acknowledgements

This research was supported by Brain Korea 21 (BK21) and KOSEF/SNU-IAMD

## References

[1] M. Ceraolo, C. Miulli, A. Pozio, J. Power Sources 113 (2002) 131–144.
[2] Y. Shan, S. Choe, J. Power Sources 145 (2005) 30–39.
[3] D. Song, Q. Wang, Z. Liu, C. Huang, J. Power Sources 159 (2005) 928–942.
[4] Y. Wang, C.-Y. Wang, Electrochim. Acta 50 (6) (2005) 1307–1315.
[5] Y. Wang, C.-Y. Wang, Electrochim. Acta 51 (2006) 3924–3933.
[6] Y. Wang, C.-Y. Wang, J. Electrochem. Soc. 154 (7) (2007) B636–B643.
[7] W. Yan, C. Soong, F. Chen, H. Chu, J. Power Sources 143 (2005) 48–56.

[8] S. Shimpalee, W.K. Lee, J.W.V. Zee, H.N. Neshat, J. Power Sources 156 (2006) 355–368.
[9] S. Shimpalee, W.K. Lee, J.W.V. Zee, H.N. Neshat, J. Power Sources 156 (2006) 369–374.
[10] S. Shimpalee, D. Spuckler, J.W.V. Zee, J. Power Sources 167 (2007) 130–138.
[11] A. Kumar, R.G. Reddy, J. Power Sources 155 (2006) 264–271.
[12] F. Mueller, J. Brouwer, S. Kang, H. Kim, K. Min, J. Power Sources 163 (2007) 814–829.
[13] S. Kim, S. Shimpalee, J.W.V. Zee, J. Power Sources 134 (2004) 110–121.
[14] S. Kim, S. Shimpalee, J.W.V. Zee, J. Power Sources 137 (2004) 43–52.
[15] S. Kim, S. Shimpalee, J.W.V. Zee, J. Electrochem. Soc. 152 (6) (2005) A1265–A1271.
[16] Q. Yan, H. Toghiani, H. Causey, J. Power Sources 161 (2006) 492–502.
[17] H. Weydahl, S.M. Holst, G. Hagen, B. Borresen, J. Power Sources 171 (2007) 321–330.
[18] S. Takaichi, H. Uchida, M. Watanabe, J. Electrochem. Soc. 154 (12) (2007) B1373–B1377.
[19] H.-S. Kim, K. Min, Visualization study of liquid water droplet dynamics related to cathode flooding with operating conditions in a PEM unit fuel cell, J. Power Sources (in preparation).